ISA Transactions ■ (■■■■) ■■■–■■■

Contents lists available at ScienceDirect

ISA Transactions

journal homepage: www.elsevier.com/locate/isatrans

Research Article

A robust adaptive load frequency control for micro-grids

Mohammad-Hassan Khooban [a,b,*], Taher Niknam [a], Frede Blaabjerg [b], Pooya Davari [b], Tomislav Dragicevic [b]

[a] Department of Electrical Engineering, Shiraz University of Technology, Shiraz, Iran
[b] Department of Energy Technology, Aalborg University, Aalborg DK-9220, Denmark

ARTICLE INFO

Article history:
Received 17 December 2015
Received in revised form
8 May 2016
Accepted 4 July 2016
This paper was recommended for publication by Oscar Camacho.

Keywords:
Adaptive PI control
General Type II Fuzzy Logic
Load frequency control (LFC)
Modified Harmony Search Algorithm (MHSA)
Micro-grids

ABSTRACT

The goal of this study is to introduce a novel robust load frequency control (LFC) strategy for micro-grid (s) (MG(s)) in islanded mode operation. Admittedly, power generators in MG(s) cannot supply steady electric power output and sometimes cause unbalance between supply and demand. Battery energy storage system (BESS) is one of the effective solutions to these problems. Due to the high cost of the BESS, a new idea of Vehicle-to-Grid (V2G) is that a battery of Electric-Vehicle (EV) can be applied as a tantamount large-scale BESS in MG(s). As a result, a new robust control strategy for an islanded micro-grid (MG) is introduced that can consider electric vehicles' (EV(s)) effect. Moreover, in this paper, a new combination of the General Type II Fuzzy Logic Sets (GT2FLS) and the Modified Harmony Search Algorithm (MHSA) technique is applied for adaptive tuning of proportional-integral (PI) controller. Implementing General Type II Fuzzy Systems is computationally expensive. However, using a recently introduced α-plane representation, GT2FLS can be seen as a composition of several Interval Type II Fuzzy Logic Systems (IT2FLS) with a corresponding level of α for each. Real-data from an offshore wind farm in Sweden and solar radiation data in Aberdeen (United Kingdom) was used in order to examine the performance of the proposed novel controller. A comparison is made between the achieved results of Optimal Fuzzy-PI (OFPI) controller and those of Optimal Interval Type II Fuzzy-PI (IT2FPI) controller, which are of most recent advances in the area at hand. The Simulation results prove the successfulness and effectiveness of the proposed controller.

1. Introduction

The entrance of DGs and MGs to the power systems results from some challenges, such as growing demand for energy, environment issues and growing reliability in power systems [1]. The complexity and uncertainty in the system are raised by these new technologies. The increase of reliability of the conventional power systems and the improvement of economic and environmental issues are the factors of the MGs entrance into the power systems [2]. For reducing global warming and increasing the speed of entering the power industry in the deregulated environments, presence of RESs in the MGs is very helpful. MGs are placed in low/medium voltage (LV/MV) levels of distribution networks [3].

Changes in system state parameters and operating conditions are fast especially in an isolated MG with fluctuant renewable sources and EVs. Traditional controllers cannot guarantee to control the system frequency in the presence of V2G and other units [4,5] because it is not optimal for the whole set of operating conditions and configurations. Moreover, generating rate and capacity constraints in the LFC units are not easy to be considered in the controller design [6]. As a consequence, in an isolated MG, a controller that performs robustly over a wide range of system operating conditions is necessary [7]. The load frequency control aims to maintain the power balance in the system such that the frequency deviates from its nominal value to within specified bounds and according to practically acceptable dynamic performance of the system [4,6]. This control strategy may be highly efficient (fuel saving) and economical since it takes advantage of minimum additional equipment and maintenance, etc.

Many controllers, such as conventional PID control [6], intelligent control [8], adaptive control [5], robust control [7], and MPC [4], have been used in order to make the LFC respond better. In [9],

Abbreviations: MG(s), micro-grids; OGT2FLC, optimal General Type-II Fuzzy Logic controller; HS, harmony search; MHSA, Modified Harmony Search Algorithm; IT2FPI, interval type-II fuzzy PI; EV, electric vehicle; GA, genetic algorithm; PSO, particle swarm optimization; PV, photovoltaic; WT, wind turbine; MPC, model predictive control; V2G, vehicle to grid; BESS, battery energy storage system; FESS, flywheel energy storage system; DMS, distribution management system; DG, diesel generator; LFC, load frequency control; FLC, fuzzy logic control; RESs, renewable energy sources; PHEVs, plug-in hybrid electric vehicles; SOC, state of charge; PMUs, phasor measurement units; FC, fuel cell; MFs, membership functions

* Corresponding author.
E-mail addresses: mhk@et.aau.dk, khooban@sutech.ac.ir (M.-H. Khooban).

http://dx.doi.org/10.1016/j.isatra.2016.07.002
0019-0578/

coordinated control of blade pitch angle of wind turbine generators and PHEVs is presented for LFC of MG using MPC. In this study, the smoothing of wind power production by pitch angle control is suggested using the MPC method and is in accordance with PHEVs control in order to decrease the number of PHEVs. In [10], in wind diesel hybrid power systems, the control system is based on a PI controller, where the index of the integral square error (ISE) was optimized for the sake of having better PI's parameters. The PI controller could not have good control performance over a wide range of operating conditions because it has been modeled at nominal operating conditions. In [4], in order to show V2G capabilities for frequency regulation and voltage sag reduction using fuzzy logic FL controller, a typical city distribution system was designed. However, this method has many drawbacks because it can show good dynamics merely when some specific membership functions were chosen. Robust H-infinity LFC for hybrid DG system has been studied in [11], the proposed method of which is too complex. In [12], small-signal stability analysis of an autonomous MG with storage system has been conducted. The new hierarchical control architecture for isolated MG is presented in [3]. Since the proposed algorithms based on aforementioned PI controller are not robust, intelligent PID controllers have been lately introduced applying/exerting FL [2,8].

Recently, researchers pay attention to general Type II fuzzy sets and systems because of their ability to deal with uncertainties and disturbances [13–23]. Zadeh in 1975 presented Type II fuzzy sets as an extension of Type I fuzzy sets [18]. Since the calculation of Type II fuzzy logic systems especially IT2FLSs are easy, they have been successfully used in engineering areas. This demonstrates the efficient performance of IT2FLSs in comparison to Type I fuzzy logic systems (T1FLS) when faced with various uncertainties such as dynamic uncertainties, rule uncertainties, external disturbances and noises [19]. Available information for making rules in a fuzzy logic system can be uncertain. Unlike interval Type II fuzzy sets (IT2FS) and Type I fuzzy sets (T1FS), general Type II fuzzy sets can deal with rule uncertainties. In the literature, since the general Type II fuzzy sets and systems are computationally complex, only IT2FLSs have been mainly applied. Liu proposed a useful fast process for computing centroid and type reduction of GT2FLS using a recent plane representation theorem [19]. In [14–18], main concepts of Type II fuzzy sets and systems were well set up. The core concept of centroid for Type II fuzzy sets was expanded by Karnik and Mendel [20]. Furthermore, an algorithm is presented which is called KM algorithm and it is used to compute the centroid of Type II fuzzy sets (T2FSs). A new representation geometric method for general Type II fuzzy sets (GT2FS) is introduced by Coupland and John [21]. But this method is beneficial for standard T2FSs and it is not useful for sets with rotational symmetry. Plane representation, a new method for GT2FSs, is introduced in 2006 by Liu [24] which is beneficial for both computational and theoretical tasks. A GT2FLS is divided into several IT2FLS with the level of for each of them by using plane representation theorem. An independent type reduction for each plane of GT2FLS was proposed by Liu in 2008.

This paper introduces a new adaptive approach using a combination of the GT2FLC logic and MHSA techniques for adaptive tuning of the most common existing PI controller based on LFC in islanded MG(s). According to the online measurements, PI parameters are tuned automatically by applying GT2FLC rules. Considering an optimal performance, the MHSA technique is used online to specify the membership functions' parameters. Unlike the classical tuning methods which are not suitable for providing a useful performance over a wide range of operating conditions, many advantages are offered by the proposed optimal tuning scheme for a MG frequency control with many distributed generations and renewable energy resources. Moreover, this proposed method is not complex in comparison to the above-mentioned methods. The simulation study is performed on a complex MG, including different loads and renewable generation resources to demonstrate the effectiveness of the proposed control scheme, and the superiority of the suggested controller over OFPI controller and OIT2FPI controllers is demonstrated in Section 6 through simulations.

The rest of the paper is organized as follows. In Section 2, the model of MG in isolated mode is defined. Then, in Section 3, the new General Type-II Fuzzy Logic formulation is completely reviewed. In Section 4, a Modified Harmony Search Algorithm is discussed in details. Section 5 shows the advantage of the proposed method in a simple flowchart. A simulation example using a specific isolated MG system under various disturbances is performed to support the functionality of the proposed control scheme in Section 6. Finally, conclusions are drawn in Section 7.

2. Model of isolated micro-grid

2.1. The micro-grid model

Fig. 1 illustrates an MG including distributed loads, low voltage distributed energy resources such as micro-turbines, WTs, PVs, and storage devices such as FESS and BESS [2].

DMS manages the power grid, and MG dispatch system (MGDS) controls the MG operation. Distributed generation resources, EV (s), loads, and PMUs are installed in this MG in order to measure the real-time information of circuit breakers [4].

2.2. Model of the electric vehicle

Using equivalent EV with different inverter capacities can handle the modeling of EVs because there are different numbers of EVs in each EV station. Fig. 2 illustrates the equivalent EV model which can be used for load frequency control [4,24]. The behavior of the battery characteristic of one EV is shown in this model, where the total charging or discharging power in controllable state can be calculated accordingly. As is mentioned, the response to the LFC signal can be limited by the number of controllable EVs and by the EV customers' convenience indicated by the specified SOC. After charging, the EV can respond to the LFC signal only within the energy capacity limit, i.e., MWh limit [4].

$$E_{control}^{min} \le E_{control} \le E_{control}^{max} \quad (1)$$

where $E_{control}$ is the total energy of the controllable EVs, while $E_{control}^{min}$ and $E_{control}^{max}$ are the lower and upper energy capacity limits, respectively. These energy capacity limits are computed from

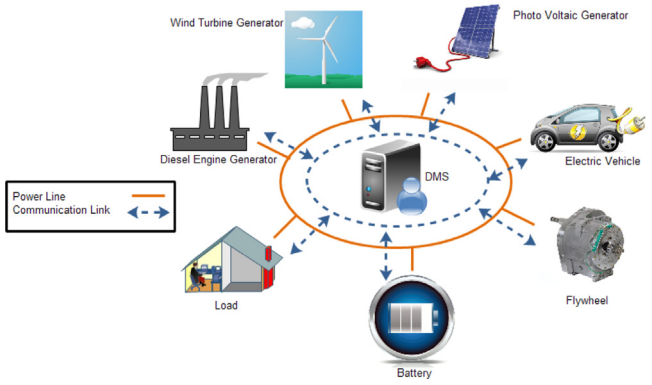

Fig. 1. General scheme of micro-grids.

Please cite this article as: Khooban M-H, et al. A robust adaptive load frequency control for micro-grids. ISA Transactions (2016), http://dx.doi.org/10.1016/j.isatra.2016.07.002

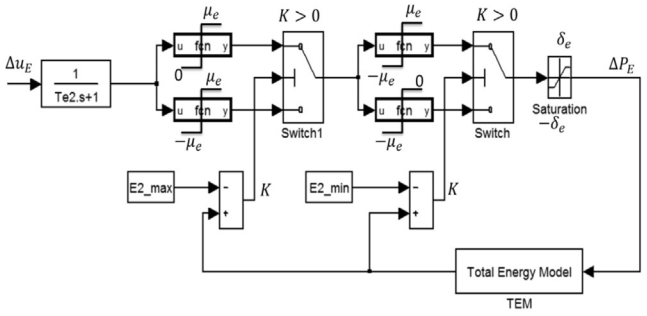

Fig. 2. The electric model in Micro-Grid LFC.

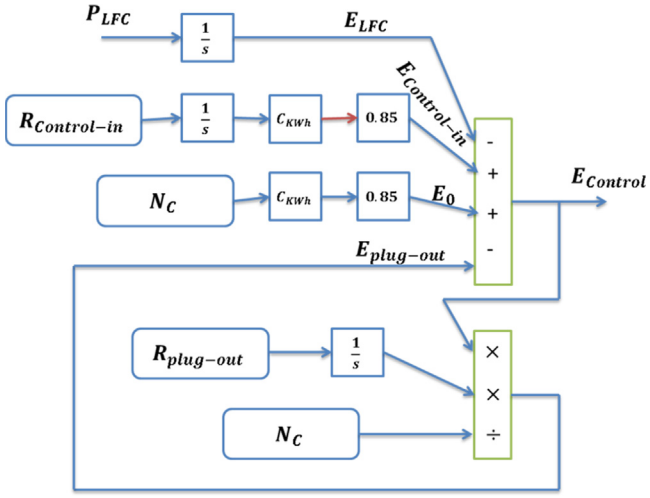

Fig. 3. Total energy model.

(2)-(3) which depend on the control strategy, i.e. the specified SOC [24,25].

$$E_{control}^{min} = \frac{N_{control} \cdot C_{kWh}}{1000} \times 0.8 \quad (2)$$

$$E_{control}^{min} = \frac{N_{control} \cdot C_{kWh}}{1000} \times 0.9 \quad (3)$$

Fig. 3 shows the total energy model which generates the total stored energy of all controllable EVs as $E_{control}$. From Fig. 3, $E_{control}$ is calculated by the following equation.

$$E_{control} = -E_{LFC} + E_{control-in} + E_0 - E_{plug-out} \quad (4)$$

where

E_{LFC}: the energy corresponding to the LFC signal
$E_{control-in}$: the energy increase due to the EVs which change the state from the charging one to the controllable one. The number here is calculated from the integral of the control-in rate, $R_{control-in}$.
E_0: the initial energy
$E_{plug-out}$: the energy decrease due to the plug-out EVs which can be computed from (5)
$N_{control}$: The number of controllable EV(s)
$R_{control-in}$: The control-in rate

$$E_{plug-out} = \frac{Z}{N} \sum_{i=1}^{N} E_i \quad (5)$$

where E_i is the energy of the i of EV, and N is the total number of EVs, Z is the number of the plug-out EVs. It's obvious that the plug-out EV has the average energy of the controllable EVs [4]. In (6) it is assumed that the plug-out EV has the average energy of the controllable EVs. Therefore, N is equal to $N_{control}$ and the sum of E_i is equal to $E_{control}$. The number of plug-out EVs is equal to the integral of the plug-out rate, $R_{plug-out}$. As a result, (6) can be rewritten as;

$$E_{plug-out} = \frac{\int R_{plug-out}}{N_{control}} E_{control} \quad (6)$$

In Fig. 2, T_e is the time constant of EV, Δu_e is the LFC signal dispatched to EV, $\pm\mu_e$ are the inverter capacity limits, and $\pm\delta_e$ are the power ramp rate limits. E_{max} and E_{min} are the maximum and minimum controllable energies of the EV battery, respectively. Finally, ΔP_E is the charging/discharging power [4]. $\Delta P_E = 0$ means EV is in idle state, $\Delta P_E > 0$ means EV is in discharging state and $\Delta P_E < 0$ means EV is in charging state. The EV can be charged and discharged only within the range of $\pm\mu_e$. However, if the energy of the EV exceeds the upper limit (i.e., E_{max}), the EV can only be discharged within the range of $(0 \sim \mu_e)$. Also, if the energy of the EV is under the lower limit (i.e., E_{min}), the EV can only be charged within the range of $(-\mu_e \sim 0)$ [24,25].

2.3. Model of the diesel power system

Diesel generator (DG) is a small scale power generation equipment with the features of fast starting speed, durability and high efficiency. DG can follow the load demand variations by power control mechanisms within short intervals [7]. When power demand fluctuates, the DG varies its output via fuel regulation. The continuous time transfer function model of the DG for LFC is shown in Fig. 4. The relationship between LFC signal and the output power of DG is represented by this model. It can be seen that this model consists of a governor and a generator, which are denoted by first-order inertia plants respectively.

In Fig. 4, Δf denotes the frequency deviation, Δu_{DG} denotes the LFC signal transmitted to DG,ΔX_G is the amount of increment in the valve position of the governor, T_g and T_d are time constant of the governor of the DG, respectively. Also, R represents speed regulation coefficient of the DG, $\pm\mu_{dg}$ are power increment limits, $\pm\delta_{dg}$ denote power ramp rate limits and ΔP_{DG} is the output power increment. $\Delta P_{DG} = 0$ represents a state in which the power generation of DG equals a is set to a value that just balances generation and load of the grid. In such circumstances, frequency deviation is zero, i.e. $\Delta f = 0$. In general, this certain output power threshold is determined by the power balance of the grid. $\Delta P_{DG} > 0$indicates that DG generated power is greater than required, while inversely, $\Delta P_{DG} < 0$ represents that the output power of DG is less than what is actually required [4].

2.4. Wind turbine model

Owing to time-variant wind direction and wind speed [2], the output power of wind turbine is fluctuant as a natural source. By

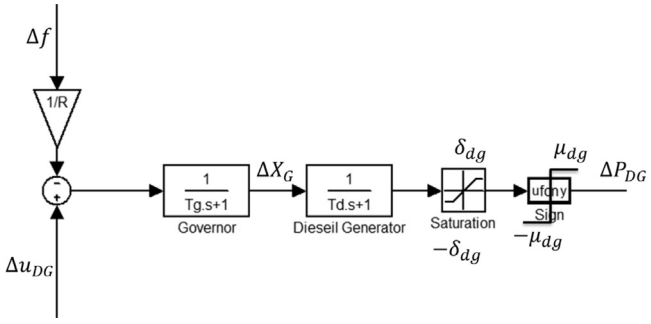

Fig. 4. Diesel power system model.

Please cite this article as: Khooban M-H, et al. A robust adaptive load frequency control for micro-grids. ISA Transactions (2016), http://dx.doi.org/10.1016/j.isatra.2016.07.002

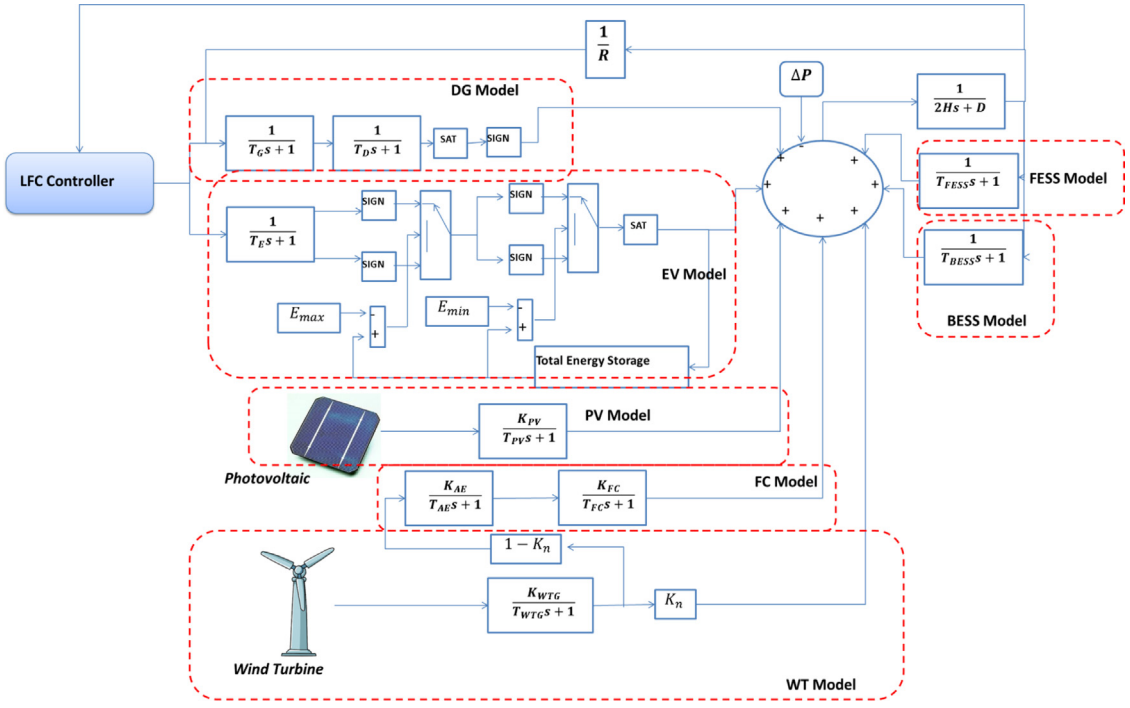

Fig. 5. Micro-Grid scheme including EV for LFC.

scrutinizing the performance of controllers for EV and DG, little effect of the inner characteristics of wind turbine on LFC of the MG is determined. Thus, in this paper [4], the wind power can be simplified as a power fluctuation source of the isolated gird. Fig. 5 shows the WT model.

2.5. Photovoltaic generation

PV cells produce power from semiconductors upon illumination. Power is produced since light is incident on the solar cell. In solar cells, the voltage loss happens because of the boundary and external contact which correlate with the shunt resistance (RS), also a small leakage current is produced because of the parallel resistance (RP). A random power source would show the photovoltaic model [2]. Intermittent power generation from wind power and photovoltaic arrays results in power fluctuation in the MG. Fig. 5 shows the PV model.

2.6. General scheme of micro-grid with LFC controller

In Fig. 6 the framework of the proposed LFC controller and the isolated MG, which includes a conventional DEG, PV panel, WTG, FC system, BESS, FESS and EV are illustrated. It is seen that power electronic interfaces which are used for synchronization in ac sources, such as DEG and WTG, and to reverse voltage in dc sources, such as PV panel, FC, and energy storage devices, connect DGs to the MG. Three fuel blocks, an inverter for converting dc to ac voltage and an interconnection device (IC) are included in FC. Although the FC has a high order characteristic, a three-order model is enough for frequency studies [2,8]. A circuit breaker is placed in each micro-source to disconnect the network and avoid the impacts of sever disturbances through the MG or for maintaining purposes. Obligatorily, the DEG produced a specific amount of power which is considered as spinning reserve for secondary frequency control (Fig. 7).

Table 1 displays the parameters of the MG power system which have been used in this study (Fig. 5) [2,4].

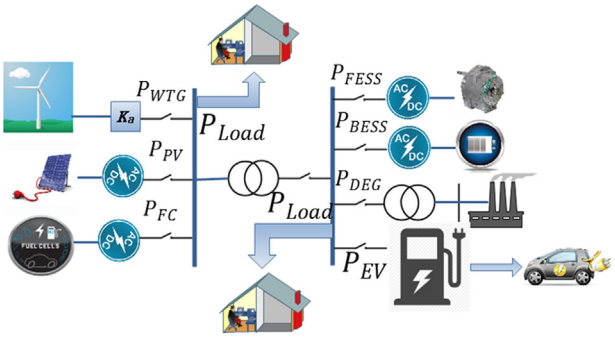

Fig. 6. Case study model for the LFC in MG system.

3. General Type II Fuzzy Systems

A GT2FLS in a universal set X can be defined as

$$\tilde{A} = \int_{x \in X} \mu_{\tilde{A}}(x)/x \tag{7}$$

$$\mu_{\tilde{A}}(x) = \int_{u \in J_x} (f_x(u))/u \quad , J_x \in [0,1] \tag{8}$$

where in (8) $\mu_{\tilde{A}}(x)$ is called a secondary MF and $f_x(u)$ is called secondary grade; J_x is the domain of the secondary MF which is called primary membership and u is a fuzzy set in [0, 1]. Fig. 4 illustrates a GT2FS where the upper and lower MFs and its secondary MF is triangular. When $f_x(u)=1$ IT2FLS is obtained that demonstrate a uniform uncertainty in the primary membership function and is simply described by its lower $\mu_{\underline{\tilde{A}}}(x)$ and upper $\mu_{\overline{\tilde{A}}}(x)$ MFs. For calculation simplicity, especially in the type reduction, many researchers use interval type-2 fuzzy sets instead of general Type II fuzzy sets [13,14,26].

Lately, Liu presented a new method for GT2FLSs which is theoretically and computationally effective [19]. Because this method resembles the α-cut for Type I fuzzy sets, it is named an α-plane for Type II fuzzy sets. $\tilde{A}_\alpha$ is the denotation of an α-plane

Please cite this article as: Khooban M-H, et al. A robust adaptive load frequency control for micro-grids. ISA Transactions (2016), http://dx.doi.org/10.1016/j.isatra.2016.07.002

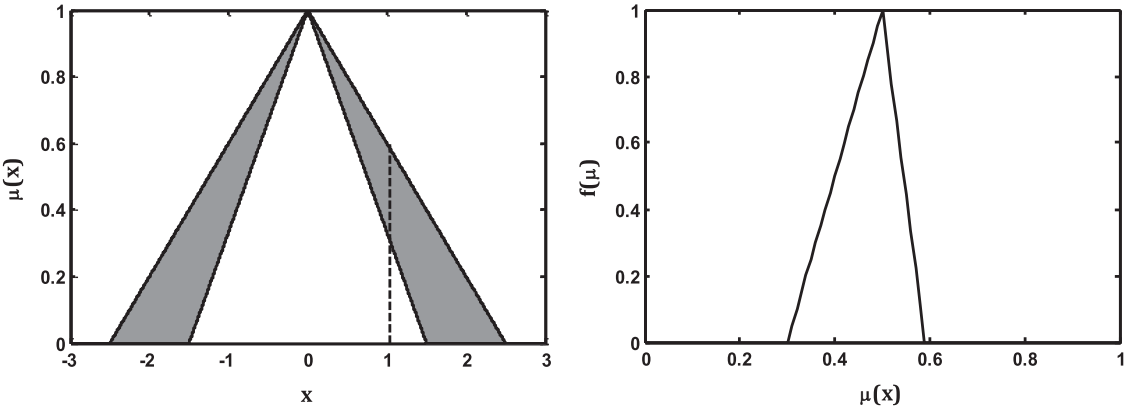

Fig. 7. General Type II fuzzy set with triangular upper and lower MFs where the secondary MF is triangular.

Table 1
MG power system's parameters.

Symbol and abbreviation	Values	Symbol and abbreviation	Values
T_g	2.000 s	T_{AE}	0.5 s
T_e	1.000 s	T_{PV}	1.8 s
R	3.000	T_{WTG}	2 s
δ_e	0.010	K_{DEG}	1/300
μ_e	0.025	K_{PV}	1
E_{max}	0.950	K_{WTG}	1
E_{min}	0.800	K_{AE}	1/500
D	0.012	K_n	0.6
2H	0.200	K_{FESS}	−1/100
T_{FESS}	0.100 s	K_{BESS}	−1/300
T_{BESS}	0.100 s	K_{FC}	1/100
T_{FC}	4.000 s	's' means second	

representation for a GT2FS $\tilde{A}$. It is the union of all primary MFs whose secondary grades are greater than or equal to the special value α:

$$\tilde{A}_\alpha = \int_{x \in X} \mu_{\tilde{A}_\alpha}(x)/x \tag{9}$$

$$\mu_{\tilde{A}_\alpha}(x) = \int_{u \in J_x} (f_x(u) \geq \alpha)/u, J_x \in [0,1] \tag{10}$$

Then a GT2FLS $\tilde{A}$ based on α-plane representation theorem can be demonstrated in the following form:

$$\tilde{A} = \bigcup_{\alpha \in [1,0]} \alpha/\tilde{A}_\alpha \tag{11}$$

It is a beneficial representation because $\alpha/\tilde{A}_\alpha$ can be seen as an IT2FS with the secondary grade of level α. As a result, several IT2FLSs may be made from the decomposition of a general Type II fuzzy set with a corresponding level of α for each, where $\alpha = \{0, 1/K, \ldots, (K-1)/K, 1\}$. In simpler terms, a general Type II fuzzy logic system can be seen as a huge collection of IT2FLSs with one IT2FLS for each value ofα. However, Liu [27] showed that using only 5 to 10 α-plane can get the required accuracy for centroid calculation. Fig. 8 illustrates the new designing for a general Type II fuzzy system based on α-plane representation.

In general, a GT2FLS is made of a fuzzifier; fuzzy rule-based; fuzzy inference engine; type reducer and defuzzifier. Fuzzifier maps real values into fuzzy sets. Singleton fuzzifier whose output is a single point of a unity membership grade is used in this paper because it is simple. Fuzzy rule base includes fuzzy IF-THEN rules. In the following The jth rule in the GT2FLS is shown:

$$R^j\text{: If } x_1 \text{ is } \tilde{F}_1^j \text{ and } x_2 \text{ is } \tilde{F}_2^j \text{ and} \ldots x_n \text{ is } \tilde{F}_n^j \text{ Then } y \text{ is } \tilde{G}^j j = 1, 2, \ldots M \tag{12}$$

where $x_i (i=1,2,\ldots,n)$ and y are the input and output of the GT2FLS, $\tilde{F}_i^j$ and $\tilde{G}^j$ are general Type II antecedent and the consequent sets. A mapping from input GT2FSs to output GT2FSs is given by the inference engine that merges rules. Because α-plane representation for fuzzy set is used, the firing set for each related IT2FLS is shown as follows:

$$F_\alpha^j(X) = [\underline{f}_{-\alpha}^j(X), \overline{f}_\alpha^j(X)] \tag{13}$$

$$\underline{f}_{-\alpha}^j(X) = \underline{\mu}_{\tilde{F}_{1\alpha}^j} * \underline{\mu}_{\tilde{F}_{2\alpha}^j} * \ldots * \underline{\mu}_{\tilde{F}_{n\alpha}^j} \tag{14}$$

$$\overline{f}_\alpha^j(X) = \overline{\mu}_{\tilde{F}_{1\alpha}^j} * \overline{\mu}_{\tilde{F}_{2\alpha}^j} * \ldots * \overline{\mu}_{\tilde{F}_{n\alpha}^j} \tag{15}$$

here $\underline{f}_{-\alpha}^j(X)$ and $\overline{f}_\alpha^j(X)$ are the lower and upper MFs of the jth rule with level of α, and * indicates product t-norm. A type reducer changes the output of the inference engine which is a Type II fuzzy set into a Type I fuzzy set before defuzzification. Five kinds of reducers which are based on calculating the centroid of an IT2FS are demonstrated in [28]. The output of the type reduction in IT2FLS is defined with its left-end point y_r and right-end point y_r due to uniformly secondary grade of IT2FLS.

KM iterative algorithms, introduced two algorithms for calculating these two end points in [28], are presented by Mendel and Karnik. In comparison to the other type reduction methods, center of sets (COS) is used a lot because of its computation simplicity by the KM iterative algorithm [20]. If singleton fuzzifier is used, product inference engine and COS type reducer, left and right end points for each part of GT2FLS based on α- representation theorem can be shown as follows:

$$y_{l_\alpha} = \frac{\sum_{j=1}^{L} \overline{f}_\alpha^j \theta_{l_\alpha}^j + \sum_{j=L+1}^{M} \underline{f}_{-\alpha}^j \theta_{l_\alpha}^j}{\sum_{j=1}^{L} \overline{f}_\alpha^j + \sum_{j=L+1}^{M} \underline{f}_{-\alpha}^j} = \theta_{l_\alpha}^T \xi_{l_\alpha} \tag{16}$$

where $\theta_{l_\alpha}^T$ is the left-end point of j^{th} consequent set with level of α, $\theta_{l_\alpha} = [\theta_{l_\alpha}^1, \ldots, \theta_{l_\alpha}^M]^T$, $\xi_{l_\alpha}^j = \left[\frac{f_{-\alpha}^j}{D_{l_\alpha}}, \frac{\overline{f}_\alpha^j}{D_{l_\alpha}}\right]$, $D_{l_\alpha} = \Sigma_{j=1}^{L} \overline{f}_\alpha^j + \Sigma_{j=L+1}^{M} \underline{f}_{-\alpha}^j$ and $\xi_{l_\alpha} = [\xi_{l_\alpha}^1, \ldots, \xi_{l_\alpha}^M]^T$. In addition,

$$y_{r_\alpha} = \frac{\sum_{j=1}^{R} \underline{f}_{-\alpha}^j \theta_{r_\alpha}^j + \sum_{j=R+1}^{M} \overline{f}_\alpha^j \theta_{r_\alpha}^j}{\sum_{j=1}^{R} \underline{f}_{-\alpha}^j + \sum_{j=R+1}^{M} \overline{f}_\alpha^j} = \theta_{r_\alpha}^T \xi_{r_\alpha} \tag{17}$$

where $\theta_{r_\alpha}^j$ is the right end point of jth consequent set with level of α, $\theta_{r_\alpha} = [\theta_{r_\alpha}^1, \ldots, \theta_{r_\alpha}^M]^T$, $\xi_{r_\alpha}^j = \left[\frac{f_{-\alpha}^j}{D_{r_\alpha}}, \frac{\overline{f}_\alpha^j}{D_{r_\alpha}}\right]$ $D_{r_\alpha} = \Sigma_{j=1}^{R} \underline{f}_{-\alpha}^j + \Sigma_{j=R+1}^{M} \overline{f}_\alpha^j$ and $\xi_{r_\alpha} = [\xi_{r_\alpha}^1, \ldots, \xi_{r_\alpha}^M]^T$. In the meanwhile, performing KM iterative algorithm can specify R and L for each individual IT2FLS of level α. From the combination of all of these obtained intervals into a Type I fuzzy set like Fig. 9, a crisp output can be obtained using centroid

Please cite this article as: Khooban M-H, et al. A robust adaptive load frequency control for micro-grids. ISA Transactions (2016), http://dx.doi.org/10.1016/j.isatra.2016.07.002

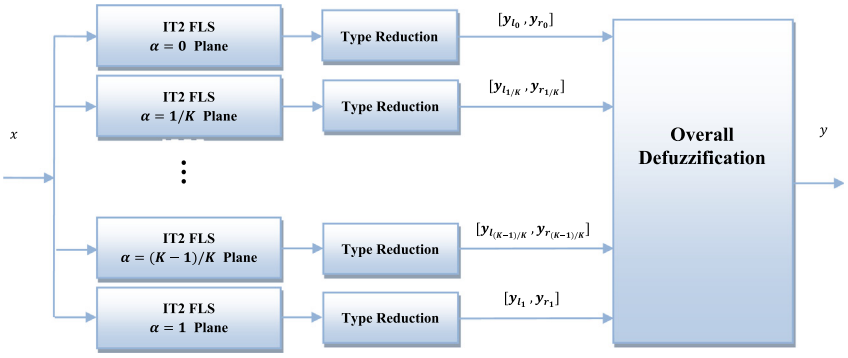

Fig. 8. Architecture for a general type-2 fuzzy Logic system.

defuzzification as:

$$U_{Fuzzy} = y = \frac{\sum_{\alpha}\alpha(y_{l_\alpha}+y_{r_\alpha})}{2\sum_{a}\alpha} = \sum_{\alpha}\alpha(y_{l_\alpha}+y_{r_\alpha})/K+1, \alpha = \left\{0.\frac{1}{K},\ldots,\frac{K-1}{K},1\right\} \tag{18}$$

where $K+1$ shows the number of the α-planes or in other words it determines the number of individual IT2FLSs.

4. Optimization technique

4.1. Original Harmony Search Algorithm

A meta-heuristic optimization algorithm, namely, the Harmony Search (HS) algorithm, inspired from the improvisation of musicians was first presented by Geem et al. [29]. The motivation to design this algorithm was to achieve musical harmony when a note is played. HS algorithm has various important aspects such as: (1) simple concept, (2) few adjusting parameters, (3) ability to solve both continuous and discrete optimization problems, (4) good tradeoff between local and global exploration and (5) easy implementation [30]. This population-based optimization algorithm begins with the production of Harmony Memory (HM) matrix. Each individual in the HM matrix indicates a note which is played by a musician in order to achieve the most harmony with other players. The improvisation process is performed on the basis of three rules: (1) memory consideration (2) pitch adjustment and (3) random research.

4.1.1. Improvisation through memory consideration and random research

A constant value called HM Considering Rate (HMCR) is determined at this stage. The use of HM and HMCR can cause the production of a new harmony as below:

$$x_{i,j}^{new} = \begin{cases} x_{i,j}^{HM}; & rand() < HMCR \\ x_{i,j}^{rand}; & Otherwise \end{cases}$$

$$X_i^{HM} = [x_{i,1}^{HM},\ldots,x_{i,d}^{HM}]$$

$$X_i^{rand} = [x_{i,1}^{rand},\ldots,x_{i,d}^{rand}] \tag{19}$$

where X_i^{HM} illustrates the ith individual in the HM matrix and X_i^{rand} is a random harmony produced in the acceptable range. As an illustration, a large value of HMCR will motivate the algorithm to construct a new harmony from the HM matrix while the low value of HMCR will motivate the algorithm to random exploration. The algorithm is motivated to create a new harmony from the HM matrix by a large value of HMCR while the algorithm to random exploration is motivated by the low value of HMCR.

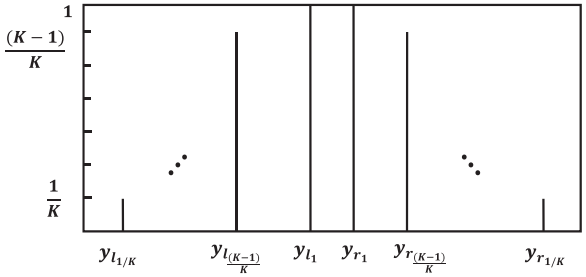

Fig. 9. Output of each individual IT2FLSs.

4.1.2. Improvisation through pitch adjustment and random research

In order to determine if the harmony produced in the last stage (Harmony Consideration) is pitch adjusted or not, it is checked. The process of pitch adjustment is patterned by determining Pitch Adjusting Rate (PAR) parameter as below:

$$x_{i,j}^{new} = \begin{cases} x_{i,j}^{rand} \pm rand \times bw; & rand < PAR \\ x_{i,j}^{rand}; & Otherwise \end{cases} \tag{20}$$

In [35], it is shown that the ability of the HS algorithm will become better by updating the value of bw, hence during the optimization process, the value of bw is updated as follows:

$$bw(g) = bw_{\max} \times \exp(\rho \times g)$$

$$\rho = Ln(bw_{\min}/bw_{\max})/NI \tag{21}$$

where $bw(g)$ denotes the bandwidth corresponding to gth iteration. Similarly, it is illustrated that updating the PAR value can improve the performance of HS algorithm [31]:

$$PAR(Iter) = PAR_{\min} + (PAR_{\max} - PAR_{\min})/NI \tag{22}$$

The HM matrix is updated when these stages passed. The improvisation process is continued until the termination criterion is fulfilled.

4.2. Modified HS Algorithm (MHSA)

In this section, a new method is suggested in order to increase the algorithm ability in local and global optimum findings. The purpose of this method is to enhance the diversity of the HM matrix when enhancing the convergence speed of the HS algorithm. Three different solutions (X_{q1}, X_{q2} & X_{q3}) are elected from HM such that $q1 \neq q2 \neq q3 \neq I$ for each solution in the HM (X_i), afterwards, a new improved solution is produced as below:

$$X_{\text{Imp}} = X_{q1} + \beta_1 \times (X_{q2} - X_{q3}) \tag{23}$$

Please cite this article as: Khooban M-H, et al. A robust adaptive load frequency control for micro-grids. ISA Transactions (2016), http://dx.doi.org/10.1016/j.isatra.2016.07.002

Now, using X_{Imp}, X_i &X_{best}, three different promising test solutions are generated as follows:

$$x^{new}_{Test1,j} = \begin{cases} x_{\mathrm{Imp},j}\,; & \beta_1 \le \beta_2 \\ x_{best,j}\,; & Otherwise \end{cases} \tag{24}$$

$$x^{new}_{Test2,j} = \begin{cases} x_{\mathrm{Imp},j}\,; & \beta_2 \le \beta_3 \\ x_{i,j}\,; & Otherwise \end{cases} \tag{25}$$

$$X_{Test3} = \beta_4 \times X_{best} + \beta_5 \times (X_{best} - HM(I_{rand})) \tag{26}$$

In the HM [31], the best individual among X_{Test1}, X_{Test2}, X_{Test3} and X_i will substitute X_i.

HMCR parameter plays a prominent role in the ability of the algorithm especially in terms of convergence speed. As mentioned above, the HS algorithm is encouraged to create a new harmony from the HM matrix by a large value of HMCR while the algorithm to random movement is encouraged by the low value of HMCR. A new formulation is determined by several running of the algorithm to update the HMCR adaptively as below:

$$HMCR^{g+1} = (1/2NI)^{1/NI} HMCR^{g} \tag{27}$$

where g shows the iteration number.

MHSA requires no information about the system. It merely needs to check the cost function for guidance of its search [32–34]. Thus, the Main Absolute Error (MAE) is shown as below:

$$MRSE = E(k) = 1/N \sum_{i=1}^{N} |e(i)| + |u(i)| \tag{28}$$

Here $e(i)$ defines the trajectory error of ith sample for the object, N defines the number of sample, i shows the iteration number and $u(i)$ is the control signal. All parameters of the GT2FLC are updated at every final time (t_f). As mentioned above, this paper studies the modeling of an adaptive PI-based controller using GT2FLC and MHSA in order to regulate frequency in MGs [2]. Fig. 10 shows the whole control framework for online adjusting of membership functions of the general Type II fuzzy rules, based on the MHSA technique.

In Table 2 the optimal performed GT2FLPI (OGT2FPI) rules are written. Membership functions which are similar to the input-output variables are collocated as Negative Small (NS), Negative Medium (NM), Negative Large (NL), Positive Small (PS), Positive Medium (PM), and Positive Large (PL), based on triangular membership function. The former parts of each rule are made, using AND function (with interpretation of minimum). Mamdani fuzzy inference system is also used. The OGT2FPI controller is more useful than other techniques as it is demonstrated in Section 6.

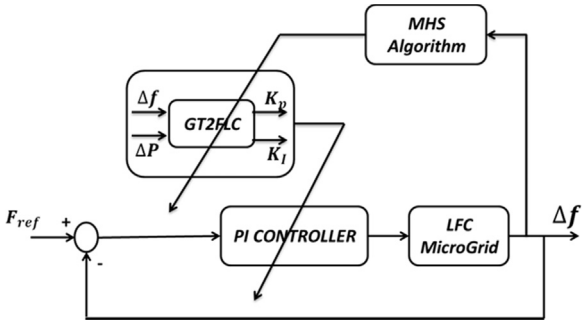

Fig. 10. General scheme of the proposed online MHSA-Fuzzy PI controller.

Table 2
The online Fuzzy PI rule set.

ΔP	Δf					
	NL	NM	NS	PS	PM	PL
S	NL	NM	NS	PS	PS	PM
M	NL	NL	NM	PS	PM	PM
L	NL	NL	NL	PM	PM	PM

5. Advantages of the proposed method

In the design of the proposed method, considerations have been made that have a prominent role in its practical implementation:

(1) The proposed novel adaptive robust control approach is easy to implement and can be applied to a reasonably wide class of MG(s).
(2) The proposed control signals are based only on the available plant input/output information and can be calculated on-line.
(3) The proposed method can be used in different configurations of MG(s), including different loads, renewable sources and grid typologies.
(4) The proposed method is free of undesirable chattering phenomena. Moreover, it can handle both structured and unstructured uncertainties.
(5) Another benefit of the proposed control approach is its light burden of computations which is an important feature in practical implementation and online control cases.
(6) A new idea of V2G is applied to use a number of small batteries of the Electric Vehicles (EVs) as an equivalent large-scale BESS, and properly control the charging and discharging of these batteries from the grid side. As a result, the required BESS capacity can be reduced.
(7) According to this matter that the Type I FLSs are unable to directly handle rule uncertainties, since their membership functions are type-1 fuzzy sets. Whereas, General Type-II FLSs involved in this paper, have capability to handle rule uncertainties. Moreover, tuning the membership function of fuzzy logic is very important to provide an optimal and accurate performance. There are several approaches toward the membership function adjustment such as trial and error and online regulating membership function method using a complementary optimization algorithm.

6. Simulation results

In this part, the module of the MG in Fig. 5 is simulated in MATLAB/Simulink environment in order to scrutinize the performance of the suggested controller. The achieved results are compared with those of Optimal Fuzzy-PI (OFPI) and Optimal Interval Type II Fuzzy-PI (OIT2FPI) controllers. The parameters of all these controllers are optimized utilizing the new MHSA optimization technique in order to represent a fair comparison. The simulation is run on a personal computer Core i5, 2.4 GHz, 8 Gbytes RAM, under Windows 7. Table 1 displays the parameters of the MG power system which have been used in this study. Fig. 11 shows the membership functions for $\alpha=0$ and $\alpha=1$. Accordingly, to construct the controller, 18 rules are required (See Table 2).

6.1. Case 1

In the first place, the load demands in the isolated mode is a constant, i.e., $\Delta P_L = 0pu$ in this case, because the output power of

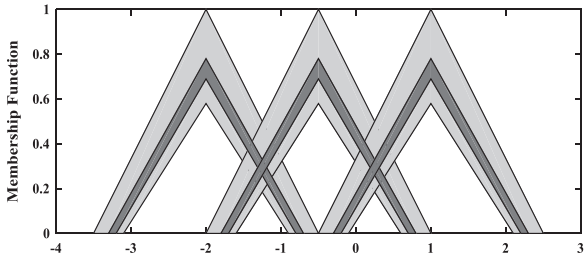

Fig. 11. General Type II fuzzy membership functions using α-plane representation with $\alpha=0$ (light area) and $\alpha=1$ (dark area).

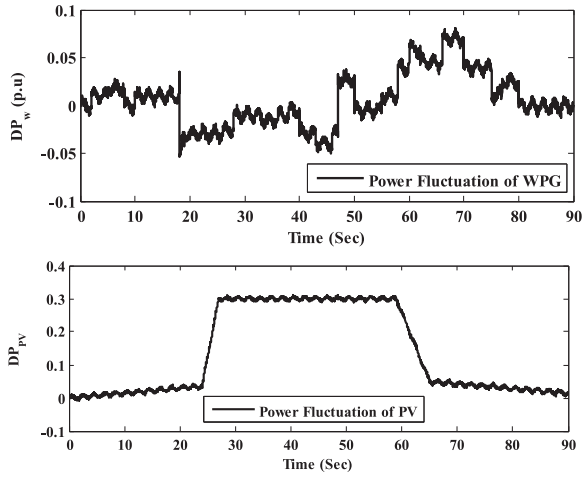

Fig. 12. Power fluctuation of WPG and PV.

WTG and PVG will fluctuate with regard to the change of weather and sun condition. Power fluctuation ΔP_w and ΔP_{pv} are used in the system. Examining Fig. 12, the data ΔP_w and ΔP_{pv} are presented which were collected from an offshore wind farm in Sweden [35] and solar radiation data in Aberdeen (United Kingdom) [36]. $\Delta P_w = 0$ and $\Delta P_{pv} = 0$ mean that wind and PV powers are respectively equal to the average wind power and irradiation power during the period. Fig. 13 illustrates the simulation result.

According to Fig. 13, the peak value in the first swing has reduced remarkably and the suggested OGT2FPI controller has quickly damped the system frequency oscillation in comparison with OFPI and OIT2FPI controllers. Furthermore, this figure illustrates that equipment life of the batteries and the DG will be longer when OGT2FPI gain stable output frequency of MG in shorter time and with less adjustment frequency. Moreover, results show that OFPI and OIT2FPI controllers have more jagged responses than the suggested controller while having a big overshoot and large settling time. Comparison of the efficiency of the OGT2FPI controller with the other two controllers reveals that the transient response is much smoother, the overshoots are less and the settling time is much smaller.

6.2. Case 2

In this part, Multi step load is considered in MG. Fig. 14 demonstrates step changes of the load in the interval of 90 seconds. The system frequency deviation using OFPI, OIT2FPI and OGT2FPI controls is shown in Fig. 15.

In Fig. 15, a better performance of the proposed intelligent control approach is obviously visible from system frequency response following first step increase in the load disturbance; and the proposed optimal controller could eliminate system frequency deviations before starting the third step increase in the load

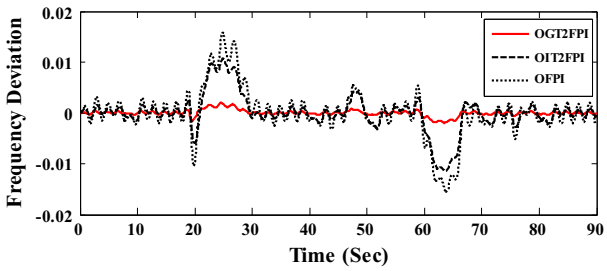

Fig. 13. Frequency response according to the power fluctuation of WPG and PV.

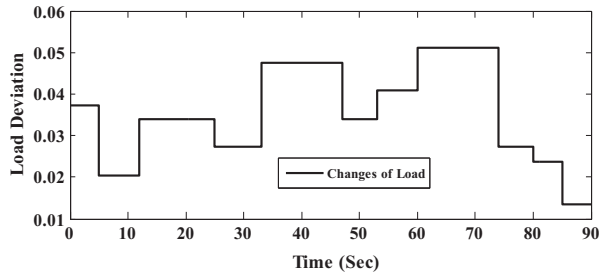

Fig. 14. Step changes of the load in the interval of 90 s.

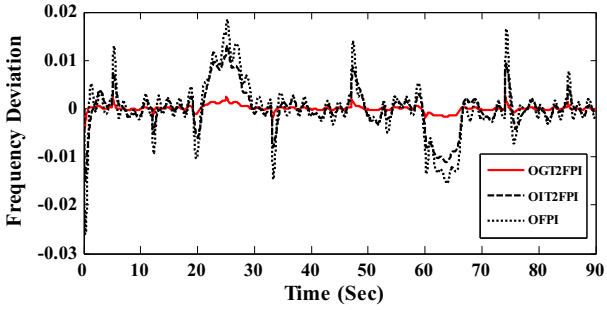

Fig. 15. Frequency response according to the power fluctuation of WPG, PV and load disturbances.

disturbance more effectively than other controllers. For the sake of comparison in a sever condition, performance of the OGT2FPI, OIT2FPI and conventional PI controllers are examined following a large step load disturbance of 60 sec, as shown in Fig. 15. In this case also, the proposed optimal control method provides a much better performance, specifically in settling time characteristic point of view.

6.3. Case 3

In the last case, in order to show the robustness of the suggested controller, some changes are made in several system parameters. Table 3 demonstrates two different scenarios of changes in system parameters with different change percentage.

According to this table, the percentage of changes used in Scenario 2 is greater than that used in Scenario 1. The frequency responses for the suggested controller, OFPI controller, and OIT2FPI controller are demonstrated in Figs. 16 and 17 respectively for each of these changes.

Frequency deviations of figures above show that the OGT2FPI controller improves the performance in comparison to the other two control structures especially in terms of overshoots. Although changes occur in system parameters in two scenarios, the performance of the suggested controller is superior to those of the two

Please cite this article as: Khooban M-H, et al. A robust adaptive load frequency control for micro-grids. ISA Transactions (2016), http://dx.doi.org/10.1016/j.isatra.2016.07.002

Table 3
Uncertain parameters of the MG system.

Parameters	Variation Range	
	Scenario 1	Scenario 2
R	+15%	+45%
D	−25%	−55%
H	+30%	+40%
T_e	−25%	−35%
T_g	+30%	+50%
T_{FESS}	−20%	−40%
T_{BESS}	+30%	−55%

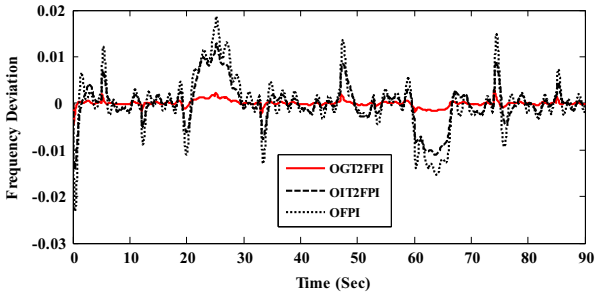

Fig. 16. Frequency deviation of the micro-grid according to Scenario 1.

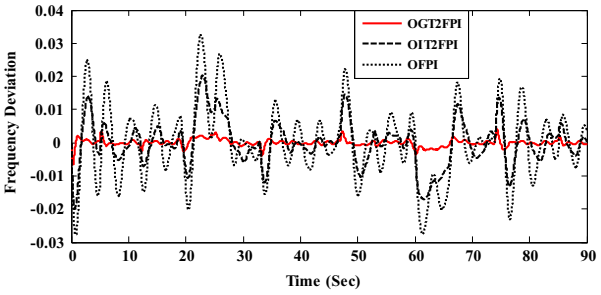

Fig. 17. Frequency deviation of the micro-grid according to Scenario 2.

controllers in Figs. 16 and 17. These figures show that the OGT2FPI controller is robust against changes in parameters.

It is obvious that the frequency response for OFPI and OIT2FPI controllers is not acceptable against the severe changes of parameters (Scenario 2) and it cannot control the MG system. Unlike other researches, this research is carried out in long term in order to keep its appropriate performance. Figs. 16 and 17 show that the control of MG system is stable in short term but not stable in long term.

7. Conclusion

In this study, a new time-varying controller based on General Type II Fuzzy Logic for LFC in an isolated micro-grid with V2G technique was presented under different operation conditions with fluctuating renewable energy generation and load disturbance. In plain language, this controller has two levels, namely, a novel General Type-II Fuzzy Logic and a conventional PI controller, which make the controller more robust. Thanks to severe dependence of the fuzzy systems on their membership functions, the new improved/modified algorithm (MHSA) is applied to improve the membership function parameters. This novel technique is computationally simple and has no complexity. According to the control model of the MG, including LFC controller, both load disturbance and the output power of the renewable source are considered as ΔP. So, the proposed controller can be used in different configurations of MG(s), including different loads, renewable sources and grid typologies. For better demonstration of the proposed control system, the results are compared with those obtained from OFPI and OIT2FPI controllers which are among the latest researches in the problem in hand.

Acknowledgements

The authors would like to thank the reviewers for their very useful comments, which helped us to improve the quality of the paper. The reviewers' efforts are gratefully appreciated. The authors wish to thank Dr. Homayounzadeh and Dr. Khalghani for their assistance in the present work.

References

[1] Greg Turner, Kelley Jay P, Storm Caroline L, Wetz DA, Lee W-J. Design and active control of a microgrid testbed. IEEE Trans Smart Grid 2015;6(1):73–81.
[2] Khalghani, Reza Mohammad, Khooban Mohammad Hassan, Mahboubi-Moghaddam Esmaeil, Vafamand Navid, Goodarzi Mohammad. A self-tuning load frequency control strategy for microgrids: human brain emotional learning. Int J Electr Power Energy Syst 2016;75:311–9.
[3] Mojica-Nava, Eduardo, Macana Carlos Andrés, Quijano Nicanor. Dynamic population games for optimal dispatch on hierarchical microgrid control. Syst, Man, Cybern: Syst, IEEE Trans 2014;44(3):306–17.
[4] Jun Yang, Zeng Zhili, Tang Yufei, Yan Jun, He Haibo, Wu Yunliang. Load frequency control in isolated micro-grids with electrical vehicles based on multivariable generalized predictive theory. Energies 2015;8(3):2145–64.
[5] Zheng S, Tang X, Song B, Lu S, Ye B. Stable adaptive PI control for permanent magnet synchronous motor drive based on improved JITL technique. ISA Trans 2013;52(4):539–49.
[6] Bevrani H, Habibi F, Babahajyani P, Watanabe M, Mitani Y. Intelligent frequency control in an ac microgrid: online PSO-based fuzzy tuning approach. IEEE Trans Smart Grid 2012;3(4):1935–44.
[7] Shiqi Zheng, Tang Xiaoqi, Song Bao, Lu Shaowu, Ye Bosheng. Stable adaptive PI control for permanent magnet synchronous motor drive based on improved JITL technique. ISA Trans 2013;52(4):539–49.
[8] Yesil Engin. Interval type-2 fuzzy PID load frequency controller using Big Bang–Big Crunch optimization. Appl Soft Comput 2014;15:100–12.
[9] Pahasa Jonglak, Ngamroo Issarachai. Coordinated control of wind turbine blade pitch angle and PHEVs using MPCs for load frequency control of microgrid. IEEE Syst J 2014;99:1–9.
[10] Mahto Tarkeshwar, Mukherjee Vivekananda. Quasi-oppositional harmony search algorithm and fuzzy logic controller for load frequency stabilisation of an isolated hybrid power system. IET Gener, Transm Distrib 2015;9(5):427–44.
[11] Singh Vijay P, Mohanty Soumya R, NandKishor, Ray Prakash K. Robust H-infinity load frequency control in hybrid distributed generation system. Int J Electr Power Energy Syst 2013;46:294–305.
[12] Lee Dong-Jing, Li Wang. Small-signal stability analysis of an autonomous hybrid renewable energy power generation/energy storage system part I: time-domain simulations. IEEE Trans Energy Convers 2008;23(1):311–20.
[13] Simon C, Robert J. Geometric Type-1 and Type-2 fuzzy logic systems. IEEE Trans Fuzzy Syst 2007;15(1):3–15.
[14] Ghaemi Mostafa, Hosseini-Sani Seyyed Kamal, Khooban Mohammad Hassan. Direct adaptive general type-2 fuzzy control for a class of uncertain non-linear systems. IET Sci, Meas Technol 2014;8(6):518–27.
[15] Khooban Mohammad Hassan, Niknam Taher, Sha-Sadeghi Mokhtar. A time-varying general type-II fuzzy sliding mode controller for a class of nonlinear power systems. J Intell Fuzzy Syst 2015:1–11.
[16] Niknam Taher, Khooban Mohammad Hassan, Kavousifard Abdollah, Soltanpour Mohammad Reza. An optimal type II fuzzy sliding mode control design for a class of nonlinear systems. Nonlinear Dyn 2014;75(1–2):73–83.
[17] Khooban Mohammad Hassan, Alfi Alireza, Abadi Davood Nazari Maryam. Control of a class of non-linear uncertain chaotic systems via an optimal Type-2 fuzzy proportional integral derivative controller. IET Sci, Meas Technol 2013;7(1):50–8.
[18] Zadeh LA. The concept of a linguistic variable and its application to approximate reasoning – I. Inf Sci 1975;8(3):199–249.
[19] Liu F. An efficient centroid type-reduction strategy for general type-2 fuzzy logic system. IEEE Comput Intell Soc , Walter J Karplus Summer Res Grant Rep 2006.
[20] Karnik NN, Mendel JM. Centroid of a type-2 fuzzy set. Inf Sci 2001;132(1-4):195–220.
[21] Coupland S, John R. A Fast Geometric Method for Defuzzification of Type-2 Fuzzy Sets. IEEE Trans Fuzzy Syst 2008;16(4):929–41.

[22] Wu H, Mendel JM. Introduction to uncertainty bounds and their use in the design of interval type-2 fuzzy logic systems. In: Proceedings of the 10th IEEE International Conference on Fuzzy Systems. San Antonio, TX, May 2000, vol. 321, p. 328–33.
[23] Mendel JM, Feilong L, Daoyuan Z. α-plane representation for type-2 fuzzy sets: theory and applications. IEEE Trans Fuzzy Syst 2009;17(5):1189–207.
[24] Masuta Taisuke, Yokoyama Akihiko. Supplementary load frequency control by use of a number of both electric vehicles and heat pump water heaters. IEEE Trans Smart Grid 2012;3(3):1253–62.
[25] Datta Manoj, Senjyu Tomonobu. Fuzzy control of distributed PV inverters/energy storage systems/electric vehicles for frequency regulation in a large power system. IEEE Trans Smart Grid 2013;4(1):479–88.
[26] Khooban Mohammad Hassan, Niknam Taher. A new and robust control strategy for a class of nonlinear power systems: adaptive general type-II fuzzy. Proc Inst Mech Eng, Part I: J Syst Control Eng 2015;229(6):517–28.
[27] Liu F. An efficient centroid type-reduction strategy for general type-2 fuzzy logic system. Inf Sci 2008;178(9):2224–36.
[28] Karnik NN, Mendel JM. Type-2 fuzzy logic systems: type-reduction. In: Proceedings of the IEEE international conference on systems, man, and cybernetics, San Diego, CA; October 1998. p. 2046–51.
[29] Geem ZW, Kim JH, Loganathan GV. A new heuristic optimization algorithm: harmony search. Simulation 2001;76(2):60–8.
[30] Ceylan H, Ceylan H, Haldenbilen S, Baskan O. Transport energy modeling with meta-heuristic harmony search algorithm, an application to Turkey. Energy Policy 2008;36(7):2527–35.
[31] Mercorelli Paolo. Parameters identification in a permanent magnet three-phase synchronous motor of a city-bus for an intelligent drive assistant. Int J Model, Identif Control 2014;5(21.4):352–61.
[32] Khooban Mohammad Hassan. Design an intelligent proportional-derivative PD feedback linearization control for nonholonomic-wheeled mobile robot. J Intell Fuzzy Syst: Appl Eng Technol 2014;26(4):1833–43.
[33] Khooban Mohammad Hassan, Niknam Taher. A new intelligent online fuzzy tuning approach for multi-area load frequency control: self adaptive modified bat algorithm. Int J Electr Power Energy Syst 2015;71:254–61.
[34] Wang Yong, Li Han-Xiong, Yen Gary G, Song Wu. MOMMOP: multiobjective optimization for locating multiple optimal solutions of multimodal optimization problems. Cybern, IEEE Trans 2015;45(4):830–43.
[35] ⟨www.winddata.com⟩ [Online; accessed 10.10.14].
[36] ⟨www.solargis.info/doc/solar-and-pv-data⟩ [Online; accessed 10.10.14].

Please cite this article as: Khooban M-H, et al. A robust adaptive load frequency control for micro-grids. ISA Transactions (2016), http://dx.doi.org/10.1016/j.isatra.2016.07.002